Constrained molecular dynamics: Simulations of liquid alkanes with a new algorithm

Cite as: J. Chem. Phys. **84**, 6933 (1986); https://doi.org/10.1063/1.450613
Submitted: 26 July 1985 . Accepted: 04 March 1986 . Published Online: 31 August 1998

Roger Edberg, Denis J. Evans, and G. P. Morriss

Constrained molecular dynamics: Simulations of liquid alkanes with a new algorithm

Roger Edberg, Denis J. Evans, and G. P. Morriss
Research School of Chemistry, Australian National University, Canberra, A. C. T. 2601, Australia

(Received 26 July 1985; accepted 4 March 1986)

We present a new algorithm for molecular dynamics simulation involving holonomic constraints. Constrained equations of motion are derived using Gauss' principle of least constraint. The algorithm uses a fast, exact solution for constraint forces and a new procedure to correct for accumulating numerical errors. We report several simulations of liquid *n*-butane and *n*-decane performed with the new algorithm. We obtain an average *trans* population of $60.6 \pm 1.5\%$ in liquid butane at $T = 291$ K and $\rho = 0.583$ g/ml. This result essentially agrees with that from an earlier simulation by Ryckaert and Bellemans [Discuss. Faraday Soc. **66**, 95 (1978)]. However, our simulations are substantially more precise; our run lengths are typically ~ 20 times longer than those of Ryckaert and Bellemans. Our result also agrees with that from a recent simulation by Wielopolski and Smith (following paper). Thermodynamic and structural data from our simulations also agree well with results from the simulations discussed in the above articles.

INTRODUCTION

Molecular fluids exhibit a vast variety of interesting physical behavior and present a challenge to theoreticians. Molecular dynamics (MD) simulation is an important tool for the study and understanding of these fluids, providing, in principle, information about anything of interest, including processes not directly amenable to experimental study. Methods for simulation of atomic fluids have been in use since the mid-1950's and are now well established. For molecular liquids, however, simulation methods are still in their adolescent stage because of the much more difficult theoretical and computational challenges they present. In this paper we describe a new algorithm for constrained molecular dynamics simulation and present results from our simulations of liquid alkanes.

In the mid-1970's Jean-Paul Ryckaert and co-workers developed the SHAKE algorithm and the "matrix method" for implementing holonomic constraints in MD simulations of complex molecules.[1] Ryckaert and Bellman's simulations of *n*-alkanes[2] were performed using both of these methods. Recently, Wielopolski and Smith[3] have performed a long simulation of *n*-butane using the SHAKE algorithm. SHAKE, originally devised for *n*-alkane molecules, has been used by many workers for simulations of molecules as large as bovine pancreatic trypsin inhibitor, a molecule composed of 58 amino acid residues.[4] In this paper we compare results from our simulations with results from Refs. 2 and 3. We do not consider results from the earliest butane simulation of Ryckaert and Bellemans[5] because these were obtained before the development of the algorithms of Ref. 1.

Our new algorithm, like SHAKE and the matrix method of Ref. 1, uses holonomically constrained equations of motion. Constraints obviate the need to follow the many irrelevant fast degrees of freedom in alkane molecules. Our algorithm contains a new and computationally efficient method of solving for constraint forces and a new procedure to correct for numerical error. A molecular thermostat, which is designed around a nonholonomic temperature constraint, is another new feature of our algorithm. Our simulation results present some new findings concerning dense liquid alkanes and clarify the SHAKE and matrix method results.

Our model alkane molecules are exactly those of Ryckaert and Bellemans in Ref. 2; each is composed of n_s sites of mass 2.411×10^{-23} g which represent the methyl or methylene groups of the alkane. Distances between neighboring sites are fixed at 1.53 Å and bond angles are fixed at 109.47° by a next-nearest-neighbor constraint. We use the same dihedral potential function to model the effect of missing hydrogen atoms on molecular conformation. Sites in different molecules and sites more than three apart on the same molecule interact through a standard 12-6 Lennard-Jones potential truncated at 2.5σ with parameters $\sigma = 3.923$ Å and $\epsilon/k = 72$ K.

This model for alkanes is useful for several reasons. First, it poses a much more challenging theoretical problem in writing and solving the equations of motion than a fully vibrational model with quadratic or Morse-type potentials for chemical bonds and bond angles. These vibrational models are easily coded. Their main drawback is the amount of computing time needed for a thorough simulation because much time is spent following fast vibrations. The constrained model eliminates these degrees of freedom and offers computational economy. This is extremely valuable when one is interested in transport processes, where the significant time scales are *vastly* longer than those for molecular vibrations.

EQUATIONS OF MOTION

Writing the equations of motion for an alkane molecule is the first and most important step in developing our algorithm. We use Cartesian coordinates for clarity. A generalized coordinate representation is quite complicated due to the many coupled internal degrees of freedom. However, with Cartesian coordinates it is perhaps not obvious how one incorporates the rigid bond and bond angle constraints into these equations.

 0021-9606/86/126933-07$02.10

Gauss' principle of least constraint[6] gives us an exact prescription for deriving equations of motion involving holonomic constraints. Constraint forces are used to maintain the desired bond distances and angles within each molecule. We will briefly illustrate how Gauss' principle is applied to obtain equations of motion for a rigid diatomic molecule and then move to the more complicated cases of *n*-butane and other *n*-alkanes.

The holonomic bonding constraint for the diatomic molecule is

$$g_{12} = \mathbf{r}_{12}^2 - d^2 = 0, \tag{1}$$

where $\mathbf{r}_{12} = \mathbf{r}_2 - \mathbf{r}_1$ and d is the desired bond length. Differentiating this equation twice with respect to time gives

$$\mathbf{r}_{12} \cdot \ddot{\mathbf{r}}_{12} + (\dot{\mathbf{r}}_{12})^2 = 0. \tag{2}$$

This equation is *central* to deriving the equations of motion for each site. Equation (2) defines a plane in either $\ddot{\mathbf{r}}_1$ or $\ddot{\mathbf{r}}_2$ space; $-\mathbf{r}_{12}$ and $\mathbf{r}_{12}$, respectively, are normal vectors. Constrained acceleration vectors must terminate on this plane. Gauss' principle states that the correct trajectory is that which minimizes the magnitude of the constraint force $\mathbf{F}_c$. Therefore, $\mathbf{F}_c$ for each atom must be a multiple of the normal vector, $\mathbf{n}$, i.e., $\mathbf{F}_c = \lambda \mathbf{n}$ with λ an undetermined scalar. Thus, the Gaussian constraint forces project the unconstrained accelerations back onto the constraint hypersurface.

The equations of motion for each site are

$$\dot{\mathbf{q}}_i = \mathbf{p}_i, \quad \dot{\mathbf{p}}_1 = \mathbf{F}_1 - \lambda \mathbf{r}_{12}, \quad \dot{\mathbf{p}}_2 = \mathbf{F}_2 + \lambda \mathbf{r}_{12}, \tag{3}$$

where site masses are set to unity. Note that the constraint forces sum to zero for the molecule. $\lambda(t)$ is determined by substituting the momentum equations of (3) into the differential constraint equation (2), giving

$$\lambda(t) = -(\mathbf{F}_{12} \cdot \mathbf{r}_{12} + \dot{\mathbf{r}}_{12}^2)/(2\mathbf{r}_{12}^2). \tag{4}$$

λ is calculated after evaluating Newtonian forces at each time step and the resulting net force, $\mathbf{F}_{\text{Newton}} + \mathbf{F}_c$, goes into an appropriate numerical method for solving the equations of motion. We have used these Gaussian equations of motion for several short trial simulations of systems of homonuclear diatomics with good results.

For an alkane molecule, the site equations of motion are of the same form as Eq. (3), except that each site is subject to coupled constraint forces. We need to calculate a set of multipliers λ_{ij} in order to solve these equations.

We obtain the equations of motion above by applying Gauss' principle of least constraint. These equations are identical, within a multiplicative constant in λ, to those derived by Ryckaert, Ciccotti, and Berendsen (RCB).[1] To solve for the multiplier we substitute the constrained equations of motion into the *differential* constraint relation (2). A *linear* equation for λ results.

Ryckaert, Ciccotti, and Berendsen follow a different procedure to obtain λ. They substitute the solution of their equations of motion for a finite time step into the *original* constraint equation (1), which gives a much more complicated equation to solve for λ. SHAKE and the matrix method of Refs. 1 and 2 are both based upon this procedure for determining constraint multipliers. Although the equations of motion are the same in both our algorithm and those of RCB, our method of calculating the constraint forces is much more straightforward.

EQUATIONS OF MOTION FOR BUTANE

Here we derive the equations of motion for a single *n*-butane molecule and outline the procedure for determining constraint forces. Site masses are set equal to unity for clarity and sites are labeled 1–4, from one end of the molecule to the other. A useful notation is $\mathbf{R}_n = \mathbf{r}_{\alpha\beta} = \mathbf{r}_\beta - \mathbf{r}_\alpha$, with $n = \alpha + \beta - 2$. This makes our equations much more compact. Note that nearest-neighbor vectors have odd n, while next nearest-neighbor vectors have even n. We write constraint forces for site α as $\lambda_{\alpha\beta}\mathbf{r}_{\alpha\beta}$, where $\alpha < \beta$.

The constrained acceleration equations for atoms one through four can be written in the form

$$\begin{pmatrix} \ddot{\mathbf{r}}_1 \\ \ddot{\mathbf{r}}_2 \\ \ddot{\mathbf{r}}_3 \\ \ddot{\mathbf{r}}_4 \end{pmatrix} = \begin{pmatrix} \mathbf{F}_1 \\ \mathbf{F}_2 \\ \mathbf{F}_3 \\ \mathbf{F}_4 \end{pmatrix} + \begin{pmatrix} -1 & -1 & 0 & 0 & 0 \\ 1 & 0 & -1 & -1 & 0 \\ 0 & 1 & 1 & 0 & -1 \\ 0 & 0 & 0 & 1 & 1 \end{pmatrix} \cdot \begin{pmatrix} \lambda_{12}\mathbf{r}_{12} \\ \lambda_{13}\mathbf{r}_{13} \\ \lambda_{23}\mathbf{r}_{23} \\ \lambda_{24}\mathbf{r}_{24} \\ \lambda_{34}\mathbf{r}_{34} \end{pmatrix},$$

or using the notation described above:

$$\ddot{\mathbf{r}}_\alpha = \mathbf{F}_\alpha + \sum_n M_{\alpha n}(\lambda \mathbf{R})_n. \tag{5}$$

The matrix M "selects" the appropriate constraints from the column vector $(\lambda \mathbf{R})_n$ for each site α.

As an example consider site number two. It is subject to three constraint forces: two from nearest neighbors one and three, and one from next-nearest-neighbor four. Its equation of motion is

$$\ddot{\mathbf{r}}_2 = \mathbf{F}_2 + \lambda_{12}\mathbf{r}_{12} - \lambda_{23}\mathbf{r}_{23} - \lambda_{24}\mathbf{r}_{24}. \tag{6}$$

Using the n notation defined above, this is

$$\ddot{\mathbf{r}}_2 = \mathbf{F}_2 + \lambda_1\mathbf{R}_1 - \lambda_3\mathbf{R}_3 - \lambda_4\mathbf{R}_4, \tag{7}$$

keeping in mind that, as in Eq. (5), the index $\alpha = 2$ applies to $\ddot{\mathbf{r}}$ and $\mathbf{F}$, and $n = 1,3,4$ to the constraint terms.

The constraint equations of motion for $\ddot{\mathbf{r}}_{\alpha\beta}$ can now be written as

$$\ddot{\mathbf{r}}_{\alpha\beta} = \mathbf{F}_{\alpha\beta} + \sum_n L_{(\alpha\beta)n}(\lambda \mathbf{R})_n, \tag{8}$$

where the matrix $L_{(\alpha\beta)n}$ is obtained by taking differences of rows β and α in M, that is, $L_{(\alpha\beta)n} = M_{\beta n} - M_{\alpha n}$. Defining a new index m analogous to n above, Eq. (8) becomes

$$\ddot{\mathbf{R}}_m = \mathbf{F}_m + \sum_n L_{mn}(\lambda \mathbf{R})_n. \tag{9}$$

To obtain a set of equations for the Gaussian multipliers we use the set of differential constraint equations equivalent to Eq. (2),

$$\mathbf{R}_m \cdot \ddot{\mathbf{R}}_m + (\dot{\mathbf{R}}_m)^2 = 0, \tag{10}$$

and substitute for $\ddot{\mathbf{R}}_m$ with Eq. (9). The result is

$$-(\mathbf{F}_m \cdot \mathbf{R}_m + \dot{\mathbf{R}}_m^2) = \sum_n (\mathbf{R}_m L_{mn} \cdot \mathbf{R}_n)\lambda_n \qquad (11)$$

which is simply a linear matrix equation that can be solved for the set λ_n once the Newtonian forces $\mathbf{F}_m = \mathbf{F}_\beta - \mathbf{F}_\alpha$ are known.

For butane there are five distance constraints. The matrices L and M are of dimension 5×5 and 4×5, respectively. For an alkane of n_s sites (carbons) there will be $n_c = 2n_s - 3$ constraints and n_c multipliers to solve for. Thus, L and M will be $n_c \times n_c$ and $n_s \times n_c$ matrices. M consists of rows in which the basic unit is [1 1 0 −1 −1] with zeros elsewhere; each successive row has this unit shifted two columns to the right. A prescription for generating M is as follows. Start by writing the basic block [1 1 0 −1 −1] in rows from top to bottom, shifting each successive row two columns to the right. Next, fill all empty spaces with zeros. Finally, trim this matrix such that its dimension is $n_s \times n_c$, ensuring that $M(1,1) = -1$ and $M(n_s,n_c) = 1$. M is the result. Knowing this, one can readily write constrained equations of motion for any n-alkane molecule.

In principle, our most difficult problem is solved. We need only incorporate the above scheme into a standard MD program in order to run simulations. However, we have overlooked a problem. Numerical errors from the inexact solution of the equations of motion and roundoff by the computer will cause the constrained distances to deviate from their desired values. In order to make our algorithm practical we need to correct for this "constraint decay" due to numerical error.

CONSTRAINT CORRECTION

To counter the effects of numerical error in the simulation, we simply readjust site positions and velocities to the proper constrained values whenever the constraints become sufficiently violated.

Consider the following penalty functions for any single constraint:

$$\Phi_n = (\mathbf{r}_{\alpha\beta}^2 - d_{\alpha\beta}^2)^2$$

and

$$\Psi_n = (\mathbf{r}_{\alpha\beta} \cdot \dot{\mathbf{r}}_{\alpha\beta})^2.$$

Φ indicates the deviation of the constrained distance from its set value while Ψ, analogous to $d\Phi/dt$, indicates how quickly the constrained distance is changing. Both Φ and Ψ should equal zero at all times if the constraint is exactly satisfied. With our equations of motion these functions increase slowly with time because of numerical error. For each molecule we define the bond penalty function Φ and the velocity penalty function Ψ as

$$\Phi = \sum(\mathbf{r}_{\alpha\beta}^2 - d_{\alpha\beta}^2)^2 = \sum(\mathbf{R}_n^2 - d_n^2)^2 \qquad (12)$$

and

$$\Psi = \sum(\mathbf{r}_{\alpha\beta} \cdot \dot{\mathbf{r}}_{\alpha\beta})^2 = \sum(\mathbf{R}_n \cdot \dot{\mathbf{R}}_n)^2, \qquad (13)$$

where the sums are over all n_c constrained distances. To correct for numerical error we minimize these potentials whenever their values become sufficiently large, adjusting positions and velocities to new values at the potential minimum. This nonlinear minimization is not nearly as expensive in computing time as one might expect. By a suitable choice of the allowed penalty function tolerances, individual molecules are never allowed to deviate very far from the true minima of Φ and Ψ. Thus the penalty function surfaces are always well behaved, positive definite and nearly quadratic.

Minimization of Φ also provides a method for constructing alkane molecules, although other methods using coordinate analysis are probably more convenient. In our simulations we have used both methods for generating starting configurations with equally good results.

THERMOSTAT

In most cases we wish to run our simulations at a specified temperature. This requires an additional application of Gauss' principle for a nonholonomic temperature constraint.[6] Note that there are many ways to define a temperature for a molecular system. For example, one could calculate a temperature using molecular center of mass velocities or atomic velocities. In either case, classical equipartition of energy equates $kT/2$ with each degree of freedom. Each constrained alkane molecule has $3n_s - n_c = n_s + 3$ degrees of freedom, and recall that MD simulations conserve the three Cartesian components of total momentum. Also, a Gaussian thermostat removes one extra degree of freedom from the system. The two temperatures are

$$T_{\text{atomic}} = \left(\sum m_{\text{site}} \mathbf{v}_{\text{site}}^2\right) \Big/ (N(n_s + 3) - 4)k \qquad (14)$$

and

$$T_{\text{molecular}} = \left(\sum m_{\text{mol}} \mathbf{v}_{\text{mol}}^2\right) \Big/ (3n - 4)k, \qquad (15)$$

where N equals the number of alkane molecules.

A Gaussian thermostat can be applied to fix either temperature,[6] giving equations of motion with an additional constraint force term $-\zeta' \mathbf{p}_{i\alpha}$ for the atomic thermostat or $-\zeta \mathbf{p}_i = -\zeta \Sigma_\alpha \mathbf{p}_{i\alpha}$ for the molecular thermostat, where index i refers to a molecule and α to atoms within molecule i. In the atomic case a large system of coupled equations for ζ' and $\{\lambda_m\}$ must be solved. These equations decouple when the themostat fixes the molecular temperature T_m; the $-\zeta \mathbf{p}_i$ terms cancel from $\ddot{\mathbf{R}}_n$ in Eq. (8). Also, the constraint forces sum to zero for each molecule. A compact expression for ζ results:

$$\zeta = \left(\sum_i \mathbf{F}_i \cdot \mathbf{p}_i\right) \Big/ \left(\sum_i \mathbf{p}_i^2\right), \qquad (16)$$

where $\mathbf{F}_i = \Sigma_\alpha \mathbf{F}_{i\alpha}$.

SIMULATION ALGORITHM

Our algorithm is now complete. We can repeatedly solve the Gaussian equations of motion for complex molecules and correct for numerical errors. After all Newtonian and dihedral forces have been calculated, a fast back-substitution routine solves Eq. (11) for each molecule, giving λ_m and thus the constraint forces. Note that complete inversion

of the matrices in Eq. (11) is unnecessary. The process of calculating the λ_m takes only a minute fraction of the total computing time, even for a system of decane molecules where L_{nm} is a 17×17 matrix. As with monoatomic simulations, the majority of computing time is spent calculating Newtonian site–site forces. A second-order Runge–Kutta procedure integrates the equations of motion. Standard periodic boundary conditions keep the molecular centers of mass within the simulation cube.

The penalty functions Φ and Ψ are monitored for each molecule at every time step and minimized if they become sufficiently large. The rate at which constraints deviate from their desired values clearly depends upon several factors, most importantly the simulation time step Δt^* and the tolerances for Φ and Ψ. We find that $\Delta t^* = 0.001$ ($\Delta t = 1.93\times10^{-15}$ s) gives good energy conservation in adiabatic test runs of the program, typically 0.1% in 10 000 time steps. The minimization routines are not called excessively with this time step. Tolerances for the penalty functions are $\sim10^{-7} > f > 10^{-12}$. Table I shows statistics: POSMIN being the minimization routine for Φ and VELMIN the routine for Ψ.

The principle difference between our algorithm and SHAKE is the method by which constraint forces are calculated. Instead of solving a *linear* matrix equation for the constraint multipliers, the SHAKE algorithm iteratively solves coupled *quadratic* equations to obtain constraint forces at each time step while keeping constraints within a specified tolerance. SHAKE effectively minimizes the penalty functions Φ and Ψ continuously. Our algorithm allows constraints to "float" slightly between tolerances which are smaller than those of SHAKE in typical applications.[1–4] The matrix solution of Eq. (11) and the minimization routines use a *very* small fraction of computing time.

We run simulations with our algorithm exactly as they are done for monoatomic liquids; we choose an appropriate starting configuration, equilibrate and then collect data of interest in a long thermostatted run. Starting configurations are cubic or fcc crystals with all dihedral angles *trans*. For our reported simulations, starting configurations were the final configurations from other runs of *at least* 50 ps, which is sufficiently long to approach *trans–gauche* equilibrium.

TABLE I. POSMIN/VELMIN statistics at state points of Ref. 2. Reduced time step = 0.001 = 0.001 93 ps. Tolerances are in reduced units (r/σ).

	Butane	Decane
Mean time between minimizations (time steps)		
1. each molecule	2300 ± 400	1800 ± 200
2. any molecule	86 ± 10	81 ± 10
Mean ΔU(system): before/after POSMIN	0.004%	0.002%
Mean $\Delta U(\phi)$: molecule minimized	0.005%	0.001%
Mean $\lvert\Delta\cos\phi\rvert$: molecule minimized	0.0003	0.0002
Minimization tolerances		
$\Phi = \sum(\mathbf{r}_{\alpha\beta}^2 - d_{\alpha\beta}^2)^2$	10^{-12}	10^{-12}
$\Psi = \sum(\mathbf{r}_{\alpha\beta}\cdot\dot{\mathbf{r}}_{\alpha\beta})^2$	10^{-13}	10^{-13}
Calling tolerances Φ and Ψ	10^{-7}	10^{-7}

Thermodynamic functions were time averaged for all of our simulations; most importantly the internal energies, pressures, and the two temperatures defined by Eqs. (14) and (15). The pressure tensor is calculated in a molecular representation.[7] Intermolecular energies are calculated from pair interactions only. Self-diffusion coefficients are calculated from mean squared displacements of the molecular centers of mass.

Molecular conformations are defined in terms of the dihedral angle ϕ:

$$\cos\phi = -\hat{\mathbf{A}}\cdot\hat{\mathbf{B}};\quad \mathbf{A} = \mathbf{r}_{12}\times\mathbf{r}_{23} \text{ and } \mathbf{B} = \mathbf{r}_{23}\times\mathbf{r}_{34}. \tag{17}$$

$\phi < (\pi/3)$ defines the *trans* state and $\phi > (\pi/3)$ the *gauche*. The "sign" of ϕ is given by the function $f_s(\phi) = \hat{\mathbf{A}}\times\hat{\mathbf{B}}\cdot\mathbf{r}_{23}$. Conformational transitions are counted at the top of the potential barrier, $\phi^* = (\pi/3)$, by checking ϕ at each time step.

SIMULATION RESULTS: BUTANE AND DECANE

Equilibrium simulations of liquid *n*-butane and *n*-decane using the new algorithm have given some new and interesting results. Table II presents these for *n*-butane at three state points. *A* and *B* correspond to states *B* 2 and *B* 1 of Ref. 2, respectively; *C* is a point not studied by MD until now. Table III shows our decane results along with those of Ref. 2. Scalar pressures [$= \frac{1}{3}\,\mathrm{Tr}(\mathsf{P})$] and intermolecular energies *are not* corrected for truncation of the site–site LJ potential.

Thermodynamics

Thermodynamic averages from our work agree well with those of Refs. 2 and 3. Dihedral potential energies differ slightly, reflecting *trans* population differences. Pressures, and intermolecular and total energies relax quickly and fluctuate about their time average values. Time averages for these variables are approximately the same at $\sim$20 ps as they are at the end of the runs.

The two temperatures show interesting behavior. T_m is rigidly fixed by the Gaussian thermostat while T_a fluctuates within $\pm\sim10\%$ of the T_m. In the initial equilibrium phase of a simulation $\langle T_a\rangle$ and T_m usually differ by quite large amounts. The agreement of $\langle T_a\rangle$ and T_m is convincing evidence that the system is truly at equilibrium.

TABLE II. Simulation results for *n*-butane — $N = 64$ molecules.

State point	*A*	*B*	*C*
Simulation time (ps)	418.52	332.93	580.90
Density (reduced)	0.419	0.365	0.365
Temperature (molecular)	2.778	4.047	5.991
Temperature (atomic)	2.817	4.122	6.065
Pressure (uncorrected)	4.046	2.637	8.242
U (dihedral)	3.050	4.613	6.434
U (intermolecular)	− 35.796	− 29.394	− 27.478
Total energy	− 22.888	− 10.345	0.182
Average percent *trans*	71.3	60.6	51.6
Ideal gas percent *trans*	78	67	58
Barrier crossings			
T–G	133	952	6284
G–T	141	955	6275
Barrier crossing rate	0.0050	0.045	0.169
$10^9\times D$ (m^2/s)	1.86	6.14	9.66

Reduced units $T^* = T/(\epsilon/k)$, $E^* = E/(N\epsilon)$, $P^* = P(\sigma^3/\epsilon)$, $\rho^* = \rho\sigma^3$
Barrier crossing rate = [transitions/simulation time (ps)]/N

TABLE III. Simulation results for n-decane — $T = 481$ K, $\rho = 0.630$ g/ml, $N = 27$ molecules.

	This work	RB (Ref. 3)
Time (ps)	55.14	19.0
Temperature (molecular)	6.680	6.68
Temperature (atomic)	6.738	...
Pressure (uncorrected)	0.298	− 0.50
U (dihedral)	45.930	*
U (intramolecular)	− 8.049	*
U (intra + dihedral)	37.881	36.03
U (intermolecular)	− 65.739	− 68.19
Total energy	15.440	13.26
$10^9 \times D$ (m^2/s)	5.15	7.5
$\langle r \rangle$	2.235	2.246
$\langle r^2 \rangle$	5.077	5.117
$\langle r^2 \rangle - \langle r \rangle^2$	0.082	0.070
Mean squared radius of gyration	0.625	0.625

Reduced units $T^* = T/(\epsilon/k)$, $E^* = E/(N\epsilon)$, $r^* = r/\sigma$, $P^* = P(\sigma^3/\epsilon)$, $\rho^* = \rho\sigma^3$, where $\rho = N/V$

Structure

The simulations give us important information about structure in dense liquid alkanes. Figures 1 and 2 show our observed site–site radial distribution functions, $g(r)$, for butane at state B and decane, respectively. Delta functions at $r/\sigma = 0.39$ and 0.63 arising from nearest- and next-nearest-neighbor constraints are omitted. For butane, the broad and sharp peaks correspond to *gauche* and *trans* conformations, respectively; the remainder of the curve shows intermolecular correlations. Decane has an even more interesting $g(r)$, with fine structure from molecular conformations; certain peaks can be attributed to conformational sequences in the molecules. The distinctive sharp peaks arise from sequences of *trans* dihedral angles. From left to right these are T, TT, TTT, and $TTTT$ at $r/\sigma = 0.98$, 1.27, 1.61, and 1.91, respectively. For these peaks, site–site distances can only be less than or equal to a maximum extension which corresponds to all of the included dihedral angles being exactly zero. Thus, they have the characteristic cusp-like shape of a "half-Gaussian" curve. The rounded peaks can be assigned to sequences with one or more *gauche* states; there are many possible sequences for each. These have full Gaussian shapes due to fluctuations about the *gauche* potential minima. Our $g(r)$ plots have the same form as those from Ref. 2, but better sampling gives us less noise at large r. This function contains much information about preferred conformations in the dense fluid.

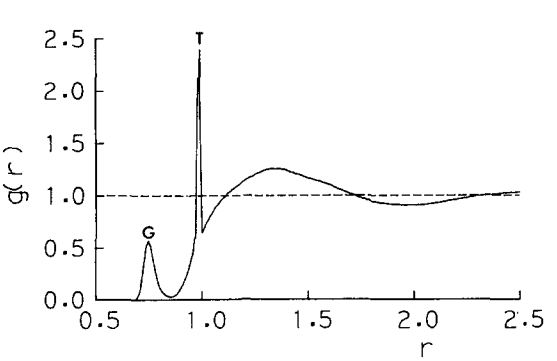

FIG. 1. Site–site $g(r)$ for n-butane at state point B, $r = r(\text{Å})/\sigma$.

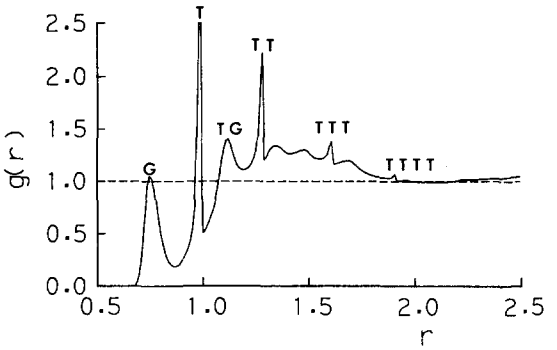

FIG. 2. Site–site $g(r)$ for n-decane, $r = r(\text{Å})/\sigma$.

Figure 3 shows our normalized distribution of end-to-end distances for n-decane. Our graph has the same shape as Ryckaert and Bellemans' distribution, but is smoother because of better sampling. This function, $ee(r)$, also has a curious fine structure from preferred conformations. Our values $\langle r \rangle$ and $\langle r^2 \rangle$ (Table III) are slightly less than those of Ryckaert and Bellemans, while our average mean squared radius of gyration agrees with their result.

$S = (1/N)\Sigma_i \hat{\mathbf{u}}_i \hat{\mathbf{u}}_i$ defines an order tensor for the system with $\hat{\mathbf{u}}_i$ an end-to-end unit vector for molecule i. For both butane and decane we observe that $\langle S \rangle = \frac{1}{3}\mathbf{I}$, indicating isotropy in the fluids at equilibrium.

Conformational equilibrium

The *trans–gauche* conformational equilibrium in dense butane has been the subject of much theoretical interest.[2,8] We find that this equilibrium shifts slightly towards the *gauche* state in going from the ideal gas to the dense fluid. From Table II, note that the average percent *trans* decreases with increasing temperature. At all three states the average population is ~6%–7% *trans* less than the prediction for molecules in the ideal gas via the expression

$$[\langle N_{\text{trans}} \rangle / N]_{\text{ideal gas}} = \int_0^{\pi/3} s^0(\phi) d\phi, \tag{18}$$

where $s^0(\phi)$ is the ideal gas dihedral distribution for constrained model butane:

$$s^0(\phi) = \exp(-V(\phi)/kT)[g^\alpha(\phi)]^{1/2} \times \left\{ \int_0^{\pi} \exp(-V(\phi)/kT)[g^\alpha(\phi)]^{1/2} d\phi \right\}^{-1}. \tag{19}$$

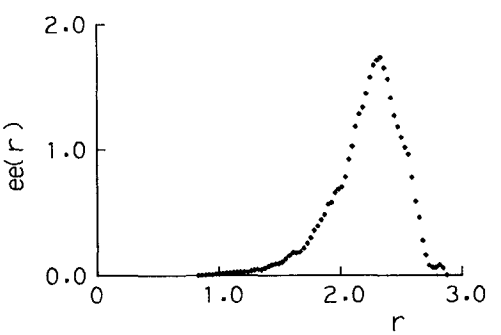

FIG. 3. Normalized end–end distribution function for n-decane, $r = r(\text{Å})/\sigma$. $r_{\max} = 2.8747$, corresponding to all dihedral angles *trans*.

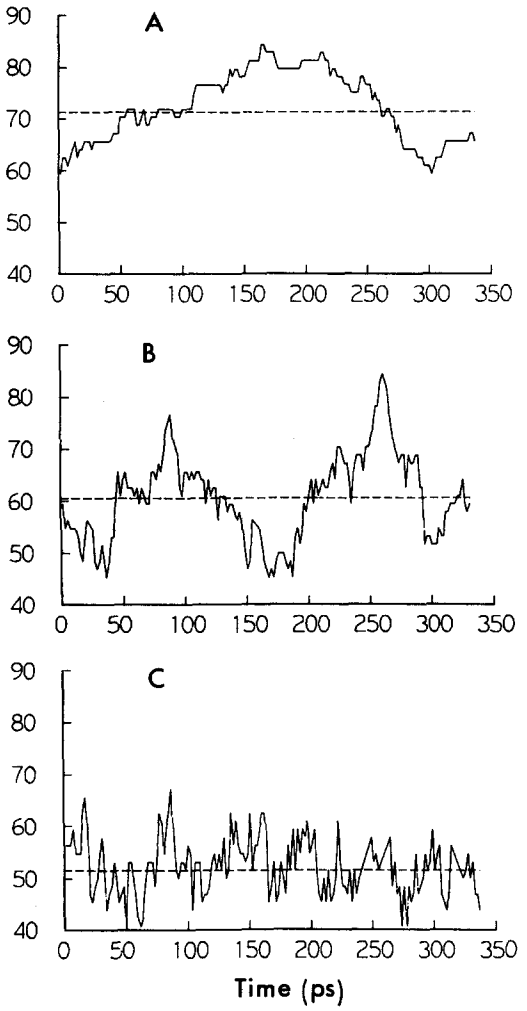

FIG. 4. Population vs time plots for state points *A*, *B*, and *C*. The horizontal lines indicate average values. Vertical axis units are percent *trans*.

$g^{\alpha}(\phi)$ is the determinant of the metric tensor for constrained model butane.[9] Figure 4 shows portions of population (percent *trans*) vs time plots for our state points *A*, *B*, and *C*; the horizontal lines indicate the average percent *trans* for each state. The three states exhibit markedly different time scales for concentration fluctuations.

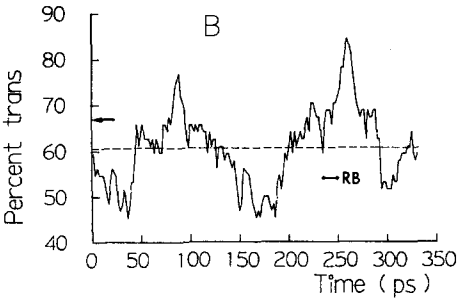

FIG. 5. Population vs time for state point *B*. The solid horizontal line (RB) covering 14 ps shows the run length and average population for Ryckaert and Bellemans' simulation. The arrow indicates the average ideal gas population.

Table IV presents our $B(=B1)$ state data and the results from Refs. 2 and 3. We are mainly concerned with our 64 molecule simulation; the small system results are included for completeness. A striking feature is the difference in real time covered by the simulations; our best run at state *B* being ~23 times as long as that of Ryckaert and Bellemans, as Fig. 5 shows.

Our most important result is an observed average population of $60.6 \pm 1.5\%$ *trans*. Wielopolski and Smith[3] obtain $58.5 \pm 1.0\%$ *trans* using the SHAKE algorithm. Ryckaert and Bellemans report an average of 54% *trans*, but do not give an error estimate. Based on run lengths, we estimate their uncertainty to be $\sim \pm 7\%$ *trans*. Thus, these three values for the equilibrium population agree. Chandler and coworkers[8] theoretically predict an average population of ~60% *trans* at the lower temperature of 274 K. At 291 K, this number should be less than 60%, possibly lying within our uncertainty. Clearly, the simulations of Ryckaert and Bellemans are much too short to give an accurate equilibrium constant for model butane.

Figure 6 shows our normalized distribution function for the dihedral angle ϕ in butane, $s(\phi)$, at state *B*. The continuous curve is the ideal gas distribution $s^0(\phi)$. Integrating our histogram curve $s(\phi)$ from $\phi = 0$ to $\pi/3$ gives exactly the same number for $\langle$% *trans*$\rangle$ as time averaging N_{trans} over the run. $\langle \Sigma_i f_s(\phi_i) \rangle = 0$, ensuring that this distribution is com-

TABLE IV. Simulation results for butane at state point $B - T = 291$ K, $\rho = 0.583$ g/ml.

	Our best simulations		RB (Ref. 2)	WS (Ref. 3)	Ideal gas
System size (molecules)	27	64	64	64	
Time (ps)	240.6	332.9	14.0	249.0	
Temperature (molecular)	4.049	4.047	4.05	3.962	
Temperature (atomic)	4.178	4.122	...	...	
Pressure (uncorrected)	5.470	2.637	1.86	0.90	
U (dihedral)	4.803	4.613	5.14	4.49	4.11
U (intermolecular)	− 27.619	− 29.394	− 30.37	− 31.42	
Total energy	− 8.194	− 10.345	− 11.06	− 13.06	
Average percent *trans*	58.1	60.6	54.0	58.5	67
Barrier crossings					
T–G	333	952	43	...	
G–T	329	955	45	...	
Barrier crossing rate	0.051	0.045	0.049	...	
$10^9 \times D$ (m^2/s)	5.05	6.14	6.1	...	

Reduced units $T^* = T/(\epsilon/k)$, $E^* = E/(N\epsilon)$, $P^* = P(\sigma^3/\epsilon)$, $\rho^* = \rho\sigma^3$, where $\rho = N/V$.
Barrier crossing rate = (transitions/simulation time (ps))/N

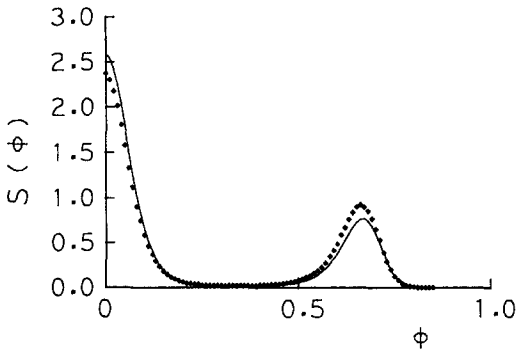

FIG. 6. Dihedral angle distributions at state point *B*. The points show our simulation distribution $s(\phi)$. The solid curve is the ideal gas distribution $s^0(\phi)$. ϕ is in units of π.

pletely symmetric about $\phi = 0$. Ryckaert and Bellemans' $s(\phi)$ *is not* symmetric about $\phi = 0$. This is further evidence that their simulated system is not fully equilibrated. At our high temperature state C ($T^* = 6.0$), $s(\phi)$ covers the entire dihedral angle space $\{0,\pi\}$, indicating at least one direct *gauche* to *gauche* transition. This is a very rare event considering that the $G \rightarrow G$ potential barrier is roughly three times as high as the $T \rightarrow G$ barrier.

Our simulations also show that classical transition state theory does not adequately describe the dynamics of isomerization in liquid alkanes. Typical trajectories along the reaction coordinate ϕ recross ϕ^* several times before settling in either the *trans* or *gauche* potential well. TST assumes that no recrossings occur. Times between recrossings in either direction for butane at state *B* are approximately normally distributed with a mean of ~ 0.20 ps; molecules recross ϕ^* two or three times on average in either direction. A simple count of barrier crossings does provide an estimate of the rate within transition state theory. However, it is not the best way to characterize a true conformational transition rate because it ignores the oscillatory nature of motion in the vicinity of ϕ^* on a short (relative to well-to-well motion) time scale and overestimates the rate constant. To more accurately describe a transition rate one could define a transmission coefficient at a given temperature and density in terms of the average number of recrossings in a long simulation. Nevertheless, our rates from a total count of barrier crossings at state point *B* are nearly identical to Ryckaert and Bellemans', despite the dramatic difference in simulation time.

CONCLUSION

We have presented a new algorithm for constrained MD simulation and results from simulations of liquid alkanes. An important advantage of this new algorithm is that constraint force multipliers are determined by solving coupled linear equations. Another advantage is the Gaussian thermostat, which allows simulation in the isothermal ensemble.[10] All previous simulations of alkanes with bond and bond angle constraints[1–3,5] have been carried out in the standard NVE or MD ensemble. Gauss' principle of least constraint plays an important role in the design of our algorithm, as it allows us to treat constraints in a clear and concise manner.

This work has been concerned with liquid *n*-alkanes, but the algorithm can easily be used for larger and more complex molecules or for different constraint schemes, nearest-neighbor bond constraints, only, for example, by changing the forms of the constraint force vector $(\lambda \mathbf{R})_n$ and the matrix **M**. Improved numerical methods and the use of vector processing could substantially decrease the computing time needed for simulations of systems of large molecules.

Agreement of results from completely different simulation algorithms, ours and those of Ryckaert and Bellemans, is very important because it essentially confirms their correctness and validity. Independent cross checks such as this are not often performed. Tildesley and Allen have recently discovered coding errors in several simulation programs from the CCP5 library.[11] Cross checking these CCP5 programs against other algorithms would have revealed the errors much earlier.

ACKNOWLEDGMENT

We gratefully acknowledge a grant of computer time under the CSIRO Merit Award scheme.

[1] J. P. Ryckaert, G. Ciccotti, and H. J. C. Berendsen, J. Comput. Phys. **23**, 327 (1977); for another description of SHAKE see W. F. van Gunsteren and H. J. C. Berendsen, Mol. Phys. **34**, 1311 (1977).
[2] J. P. Ryckaert and A. Bellemans, Discuss. Faraday Soc. **66**, 95 (1978).
[3] P. A. Wielopolski and E. R. Smith, J. Chem. Phys. **84**, 6940 (1985).
[4] W. F. van Gunsteren, H. J. C. Berendsen, F. Colonna, D. Perahia, J. P. Hollenberg, and D. Lellouch, J. Comput. Chem. **5**, 272 (1984).
[5] J. P. Ryckaert and A. Bellemans, Chem. Phys. Lett. **30**, 123 (1975).
[6] K. F. Gauss, J. Reine Angew. Math. **IV**, 232 (1829); D. J. Evans, W. G. Hoover, B. H. Failor, B. Moran, and A. J. C. Ladd, Phys. Rev. A **28**, 1016 (1983); D. J. Evans and G. P. Morriss, Comput. Phys. Rep. **1**, 297 (1984).
[7] A. J. C. Ladd, Mol. Phys. **53**, 459 (1984).
[8] D. Chandler, Discuss. Faraday Soc. **66**, 184 (1978); L. R. Pratt, C. S. Hsu, and D. Chandler, J. Chem. Phys. **68**, 4202 (1978).
[9] M. Fixman, Proc. Natl. Acad. Sci. U. S. A. **71**, 3050 (1974); W. F. van Gunsteren, Mol. Phys. **40**, 1015 (1980).
[10] G. P. Morriss and D. J. Evans, Mol. Phys. **54**, 629 (1985).
[11] D. J. Tildesley and M. P. Allen, CCP5 Q. **16**, 46 (1985).